boundary conditions for the VLTI. A number of interferometers with comparatively small aperture are already producing data or will come into operation very soon. In addition, instruments with sensitivity comparable to the VLTI (the Keck, LBT, and Magellan interferometers) may see first light soon after the VLTI. And finally, plans for interferometric space missions have been on the drawing board for quite a while. With that many contenders in the starting blocks, the competitiveness of the VLTI will depend critically on timing during all stages of its implementation. And because of its strong influence on the sensitivity, the availability of adaptive optics is an extremely important factor in this calculation.

The VLTI and Beyond

It will still take a few years until the VLTI becomes operational, and even longer before its full potential gets realised with the combination of the four 8-m telescopes using high-order adaptive optics. Nevertheless, a look ahead into the more distant future should be useful. It appears that the VLTI will be close to the limit of what can be done sensibly from the ground. Other instruments will have somewhat longer baselines, or better *uv* coverage, but it is difficult to envisage an affordable way of obtaining significantly more sensitivity, accuracy, wavelength flexibility or sky coverage than provided by the VLTI. On the other hand, interferometry from above the atmosphere looks very promising. Space is quiet, empty, and cold. In the absence of atmospheric fluctuations, the coherent integration time on any point in the sky is only limited by the observing time available, giving an enormous boost to sensitivity even with moderate (1-m-class) apertures. At $\lambda \gtrsim 2.5$ μm, the advantage of space is even larger, because the whole telescope can be radiatively cooled to a temperature of 40 K or so. The undistorted wavefront facilitates the calibration of the visibilities and makes advanced techniques for high-contrast observations feasible. Interferometer concepts based on "free flyers" – where each telescope is mounted on an independent small satellite – make very long baselines possible and provide superb imaging quality because the *uv* plane can be covered effectively. Bearing all this in mind, it seems plausible that the next big step after the VLTI will be the leap into space. Should ESO play a role in this adventure? There are very good arguments for an ESO involvement in space interferometry. First, the VLTI offers unique opportunities for the development of instrumental concepts and techniques, which have to be tested on the ground before they can be incorporated into space missions. Second, the VLTI will play an important role in defining the key scientific topics that can be addressed with space-based interferometry. And third, the efficient use of a space facility will require a user community well trained in interferometric observations. It thus appears that some coordination between ESO and ESA could be beneficial for both sides. A panel discussion with representatives of both agencies that took place during the workshop was devoted to the question of how a joint effort in the area of interferometry could work. Differences between ESO and ESA in their member nations, organisational structure, and scientific communities to be served will have to be addressed in order to define the scope and terms of a fruitful collaboration. With ESO's VLTI back on the track to fast implementation, and an interferometric cornerstone in ESA's Horizon 2000+ programme, there is an enormous potential for a strong European role in the development of interferometry. Generating synergism between these programmes can only make them stronger. We can thus look forward to exciting opportunities, and to a rich harvest of astronomical results in the near future and in the decades to come. George Miley boldly predicted that the IAU will hold its third (!) symposium on "Optical Interferometry of AGN" in November 2010. I look forward to seeing his paper at that conference, and to many other results at the meetings that will be held on imaging of T Tauri disks, stellar surface features, spectroscopy of extrasolar planets . . .

Acknowledgements

All workshop participants deserve applause for their careful preparation and enthusiastic presentations. I had the pleasure of sharing with Jean-Marie Mariotti the task of summarising the workshop in the concluding talk. I hope that some of his insight has found its way into this report.

References

ESO (1989), VLT Report No. 59.
ESO (1992), VLT Report No. 65.
Paresce, F., et al. (1996), The Messenger **83**, 14.
Walsh, J.R., and Danziger, I.J. (1995), Science with the VLT, Springer-Verlag.
Whitney, A.R., et al. (1971), *Science* **173**, 225.

Andreas Quirrenbach
e-mail: qui@MPA-Garching.MPG.DE

Simulations of VLTI/VISA Imaging Observations of Young Stellar Objects at 2.2 μm

N. AGEORGES, O. VON DER LÜHE, ESO

1. Introduction

The study of star and planet formation is one of the most exciting science goals of the VLT Interferometer. Circumstellar disks related to star and planet formation are believed to be a common feature of both young and main-sequence stars in different stages of development (e.g. Beckwith & Sargent, 1993, Backman & Paresce, 1993).

The search for direct evidence of disks around young stellar objects has been successful only recently (McCaughrean et al., 1996), although their presence has been inferred indirectly for more than a decade. Direct detection was possible only with high angular resolution observing techniques, in particular with the HST. However, much higher resolution than available with HST is needed in order to probe the structure of these disks and to test current models which predict gaps and traces of planetesimals.

In an effort to understand the science performance of the VLTI, we have studied the potential of the VISA mode to do this kind of observations by computer simulations. Our main concern is the synthesis capability of various VISA configurations. To limit the large variety of parameters, we have concentrated here on the study of a limited sample of disk morphologies at high angular resolution. We used the CalTech VLBI software package (Pearson, 1991) for our simulations.

2. Source Models

To make the computations more realistic we used disk parameters as derived from HST observations. The simulated object is located at 440 pc and corresponds to disk 182–332 of McCaughrean et al. (1996), with the exception that the declination is –30°. At this distance,

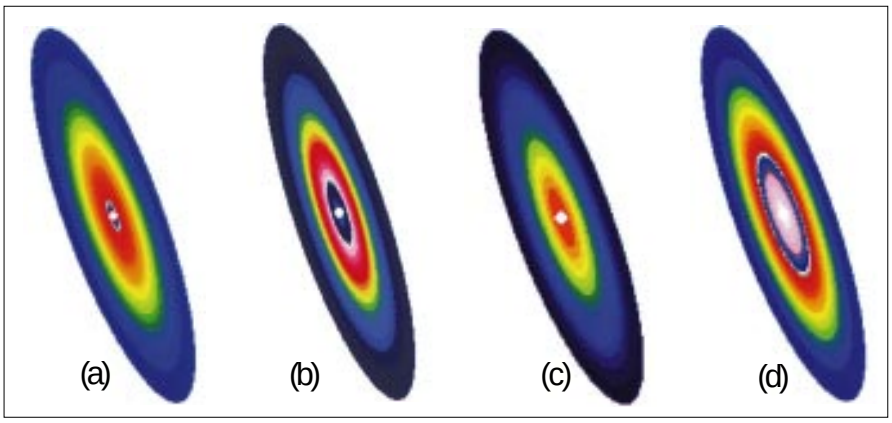

Figure 1. Simulated star + disk models: star + disk with a gap (5 AU (a); 10 AU (b), simple star + disk model (c), star + disk with a void ring (d).

the disk with a FWHM of 26 AU has an apparent extent of 60 mas. Adopting a star magnitude m_K of 9.49 and a disk luminosity of 0.5 L_*, we constructed the 4 following models:

(1) a featureless disk with an exponential intensity profile and a central unresolved source, viewed with an inclination angle of 75° ("star + disk" model),

(2) a star + disk model as above with a gap of 5 AU between the star and the inner boundary of the disk,

(3) same as before, but with a gap of 10 AU,

(4) a star + disk system with a void between 12 and 20 AU from the star.

The VLBI package allows to model sources with various mathematical

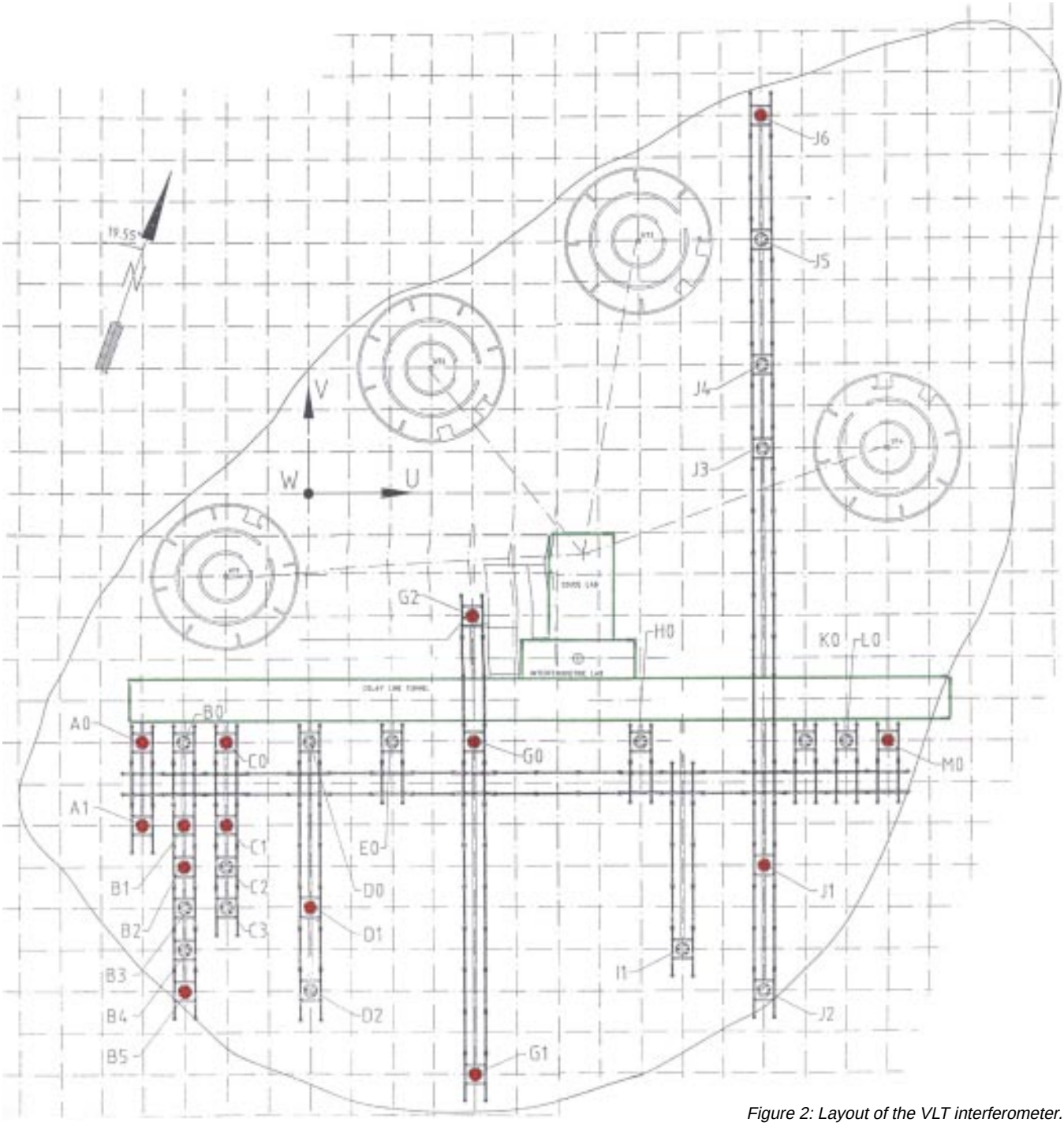

Figure 2: Layout of the VLT interferometer.

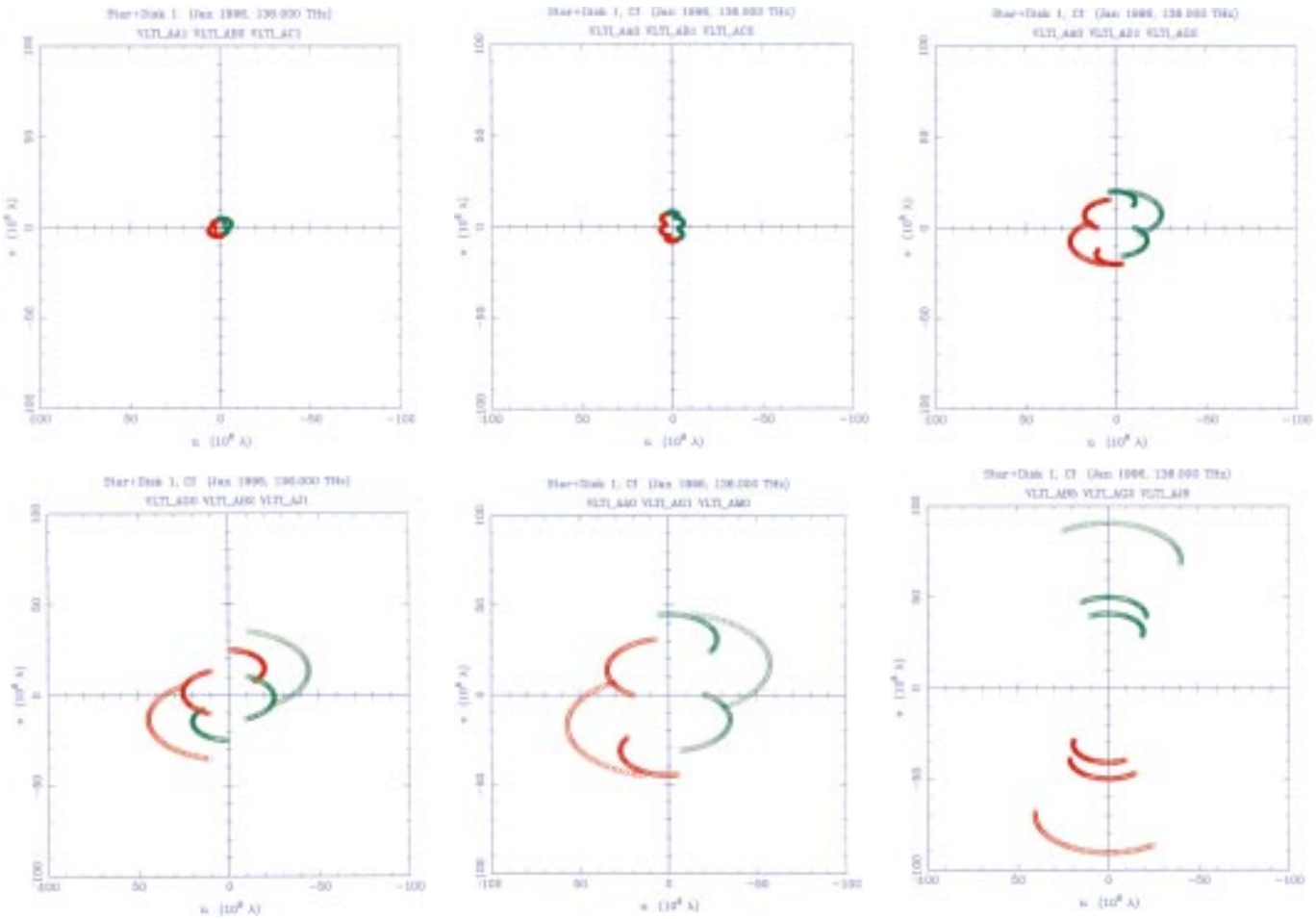

Figure 3: UV coverage from the different configurations used.

shapes, but we have used only elliptical Gaussians and uniform ellipsoids. Details of the model components are shown in Table 1.

3. Simulation of VLTI Observations

We used the actual layout (Fig. 2) for 8-m Unit and 1.8-m auxiliary telescopes of the VLT Observatory on Cerro Paranal for the modelling.

All simulations have been done for the K band at 2.25 µm, using 3 auxiliary telescopes at any given time. The integration time on source is 5 minutes, which is repeated after 10 minutes; this allows for another interleaved set of reference source integrations of approximately 5 minutes. Observations are carried out between 03:00:00 and 21:00:00, with the source culminating at 12:00:00. This corresponds to a night where the source culminates at midnight. The hour angle is then limited by the zenith distance limits of the telescopes (60°). Noise sources are photon noise and a low level of detector read-out noise (5e^-/pixel). No other phase noise sources were accounted for.

The star with an apparent diameter of 1 mas is essentially unresolved even with the longest baselines, while the disk is clearly seen only with the shortest 8-m

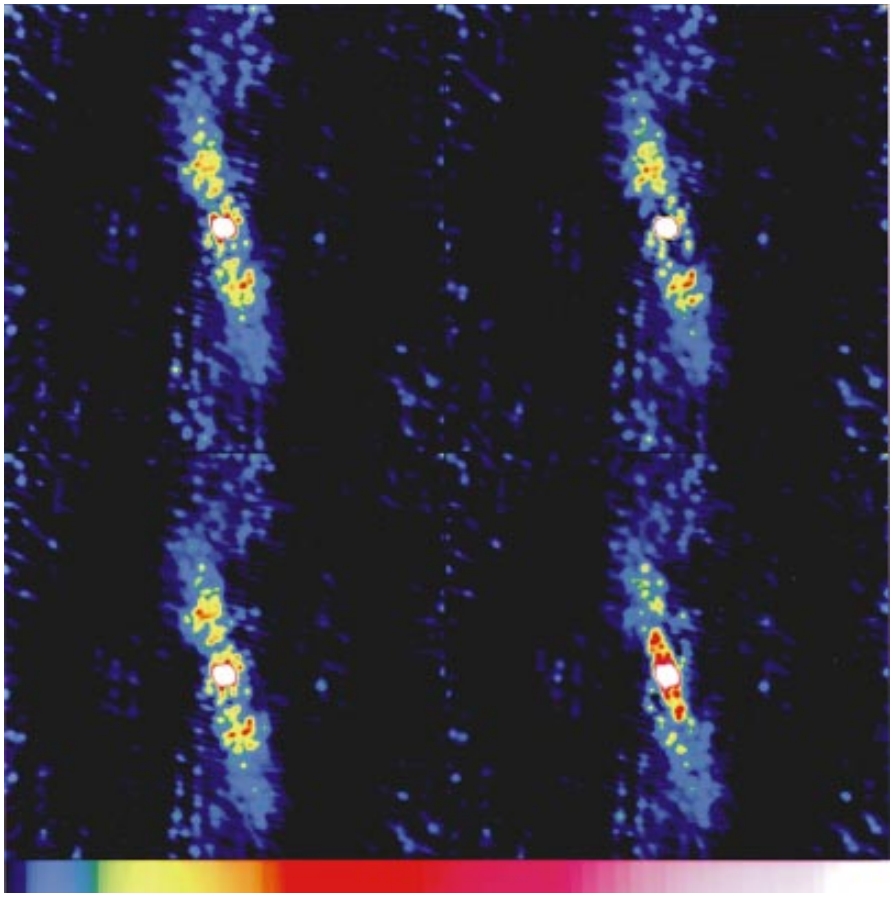

Figure 4: CLEANed images of the 4 simulated disks.

baselines between auxiliary telescopes. In fact, the disk would even be resolved with an 8-m Unit telescope with a near-infrared optimised adaptive optics system. However, the signatures of the disk features appear best at intermediate baselines of order 20 m. We therefore used six configurations of three auxiliary telescopes, the measurements of which were merged to result in a single data set which was subject to hybrid mapping and model fitting. The UV coverage of the six configurations are shown in Figure 3.

Synthetic visibility data were gridded, inverted to yield dirty maps and beams, and were subject to typically 1000 iterations of CLEAN. The resulting CLEAN maps are shown in Figure 4. We used these maps as a starting point to identify the approximate orientation and inclination angle of the disk "by eye", as well as any discernible other feature like the central gap and the ring. From these observations, initial models for the CalTech non-linear least-squares model-fitting process were constructed. The resulting final models are then compared with the original sources.

4. Results and Discussion

Table 2 shows the parameters for the initial model (as derived from the CLEAN maps) and the iterated parameters after model fitting. These should correspond to the original parameters shown in Table 1. It also shows the agreement factors (reduced Chi-squared value for the goodness of fit between the model and the data). These numbers should be small for a good fit.

The CLEAN maps of the 10 AU gap as well as the void ring do in fact show structural differences compared to the featureless disk. For the case of a 5 AU gap, the CLEAN map is indistinguishable from that of the featureless disk. We therefore excluded this case from further discussion.

The CLEAN maps reveal that the simple approach using Fourier inversion and CLEANing is inappropriate for studying extended objects like the disk since CLEAN tries to decompose any source into a collection of point sources. At best, these maps can serve as an input for constructing initial models, as we have done.

Initial model parameters can deviate substantially from the "true" values. In most cases studied, a reasonable input model would result in a final model which describes the actual source quite well after 40 iterations. Some parameters, in particular those related to the features in the disk, are quite sensitive. We could not obtain convergence of model fitting when entering a positive component brightness for those compo

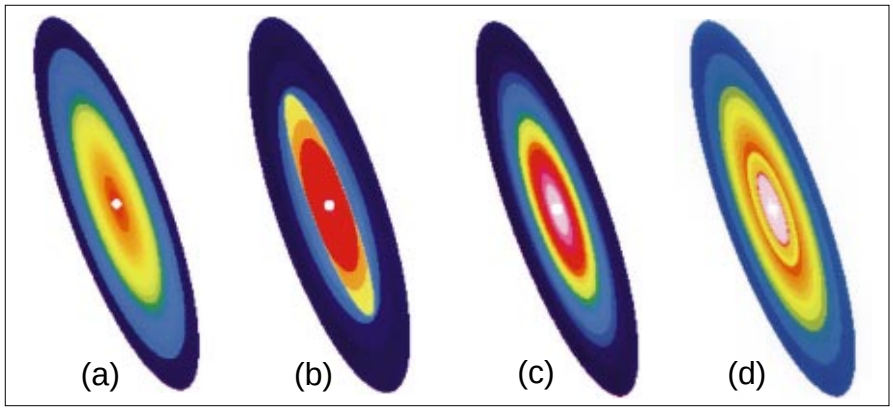

Figure 5: Results of model fitting (see Fig.1)

TABLE 1. Parameters of the different disk models studied. Definition of the type of components: 1 = elliptical Gaussian, 2 = elliptical disk of uniform brightness.

Flux (Jy)	Major Axis FWHM (mas)	Axial Ratio	Position Angle	Type
Model 1: Star disk of uniform brightness				
0.0085 0.0042	1.0000 60.0000	1.0000 0.2500	0.0000 20.0000	1 1
Model 2: Star plus disk with central void (5 AU large)				
0.0085 0.0042 –0.0001	1.0000 60.0000 11.3636	1.0000 0.2500 0.2500	0.0000 20.0000 20.0000	1 1 2
Model 3: Star plus disk with central void (10 AU large)				
0.0085 0.0042 –0.00035	1.0000 60.0000 22.7272	1.0000 0.2500 0.2500	0.0000 20.0000 20.0000	1 1 2
Model 4: Star plus disk with the trace of a planetesimal between 12 and 20 AU				
0.0085 0.0042 –0.00112 0.00105	1.0000 60.0000 45.0000 30.0000	1.0000 0.2500 0.2500 0.2500	0.0000 20.0000 20.0000 20.0000	1 1 2 2

Table 2. Parameters of the initial and iterated models.

Flux (Jy)	Major Axis FWHM (mas)	Axial Ratio	Position Angle
Initial model 1			
0.0100 0.0070	1.0000 83.8000	1.0000 0.1500	0.0000 30.0000
Model 1: Iterated parameters, agreement factor 1.067			
0.0085 0.0044	1.0000 60.3236	1.0000 0.253451	0.0000 20.1104
Initial model 3			
0.0100 0.0100 –0.0010	1.0000 70.8000 22.7270	1.0000 0.3300 0.1000	0.0000 13.9000 16.7000
Model 3: Iterated parameters, agreement factor 1.166			
0.0085 0.0043 -0.0005	1.0000 56.1651 26.2960	1.0000 0.25812 0.24544	0.0000 20.2088 19.8638
Initial model 4			
0.0100 0.0005 –0.0010 0.0050	1.0000 74.0000 39.9000 28.0000	1.0000 0.2000 0.2000 0.2000	0.0000 12.7000 15.2500 17.15000
Model 4: Iterated parameters, agreement factor 1.203			
0.0085 0.0043 0 0005 0.0008	1.0000 66.3553 44.2581 27.8947	1.0000 0.25155 0.27248 0.24074	0.0000 20.0408 19.9609 19.6639

nents which appear dark (i.e., with a negative flux) in the truth model. On the contrary, it hardly matters which initial flux is taken for the large disk component, it will always converge close to its truth value. Figure 5 shows the iterated models derived from model fitting; this should be compared to the simulated disks (Fig. 1).

Of course, this study is somewhat biased, because of the prior knowledge of the researchers, there was no "blind test". However, we made an attempt to fit the void ring model just with two components (star and large disk). Here, model-fitting convergence was slow although the two components were fairly well represented after 120 iterations. Also, the agreement factor was significantly larger (2.378). The fine structure, like the void ring, is not recovered by the model alone, i.e. the model fitting process fits to the best the parameters that were introduced as input. It does not account for a possible further component. Nevertheless we conclude that there are some objective means which would reveal an inaccurately composed model.

We also tried reducing the number of configurations, with little encouraging results. With too few baselines, one would have been unable to identify structures in the disks without prior knowledge. Using only the long baselines, recovers only the central star – the long baselines, of course, constrain only the star. We therefore conclude that it takes quite some investment in observing time to find structures in circumstellar disks.

References

Backman, D. E.; Paresce, F. (1993): in *Protostars and Planets III*, ed. G. Levy and J. Lunine, (Tucson University of Arizona Press), pp. 1253–1304.

Bechwith, S.V.W.; Sargent, A.I. (1993): in *Protostars and Planets III*, ed. G. Levy and J. Lunine, (Tucson University of Arizona Press), pp. 521– 541.

McCoughrean, M.J.; O'Dell, C. R. (1996): *A.J.* **111**, p. 1977ff.

Pearson, T. J. (1991): Introduction to the Caltech VLBI Programs, California Institute of Technology.

Nancy Ageorges
e-mail: nageorge@eso.org

On September 19, an important milestone in the VLT project was reached: the completion of the 4th 8.2-m primary mirror blank by the Schott Glaswerke in Mainz. Following a press meeting at the Erich Schott Centre, about 100 guests gathered in the large factory hall to celebrate this achievement and to have a last look at the impressive Zerodur blank before its boat journey to France. Photographs: H. Zodet